Article

BCL7C suppresses ovarian cancer growth by inactivating mutant p53

Canhua Huang[1,2,†], Qian Hao[3,4,†], Getao Shi[5], Xiang Zhou[3,4,*], and Yu Zhang[1,2,*]

[1] Gynecological Oncology Research and Engineering Center of Hunan Province, Changsha 410008, China
[2] Department of Gynecology, Xiangya Hospital, Central South University, Changsha 410008, China
[3] Fudan University Shanghai Cancer Center and Institutes of Biomedical Sciences, Fudan University, Shanghai 200032, China
[4] Key Laboratory of Breast Cancer in Shanghai, Fudan University Shanghai Cancer Center, Fudan University, Shanghai 200032, China
[5] School of Life Sciences, Shaoxing University, Shaoxing 312000, China
[†] These authors contributed equally to this work.
[*] Correspondence to: Xiang Zhou, E-mail: xiangzhou@fudan.edu.cn; Yu Zhang, E-mail: xyzhangyu@csu.edu.cn

Edited by Zhiyuan Shen

B-cell CLL/lymphoma 7 protein family member C (BCL7C) located at chromosome 16p11.2 shares partial sequence homology with the other two family members, BCL7A and BCL7B. Its role in cancer remains completely unknown. Here, we report our finding of its tumor-suppressive role in ovarian cancer. Supporting this is that BCL7C is downregulated in human ovarian carcinomas, and its underexpression is associated with unfavorable prognosis of ovarian cancer as well as some other types of human cancers. Also, ectopic BCL7C restrains cell proliferation and invasion of ovarian cancer cells. Consistently, depletion of BCL7C reduces apoptosis and promotes cell proliferation and invasion of these cancer cells. Mechanistically, BCL7C suppresses mutant p53-mediated gene transcription by binding to mutant p53, while knockdown of BCL7C enhances the expression of mutant p53 target genes in ovarian cancer cells. Primary ovarian carcinomas that sustain low levels of BCL7C often show the elevated expression of mutant p53 target genes. In line with these results, BCL7C abrogates mutant p53-induced cell proliferation and invasion, but had no impact on proliferation and invasion of cancer cells with depleted p53 or harboring wild-type p53. Altogether, our results demonstrate that BCL7C can act as a tumor suppressor to prevent ovarian tumorigenesis and progression by counteracting mutant p53 activity.

Keywords: BCL7C, mutant p53, apoptosis, invasion, ovarian cancer

Introduction

TP53 is the most frequently mutated tumor suppressor gene in cancer. Among these mutations, ∼74% are missense mutations that often occur in the DNA-binding domain (DBD) of p53, including several hotspot mutations at the amino acids R175, R245, R248, R249, R273, and R282 (Freed-Pastor and Prives, 2012; Zhou et al., 2019). Whereas wild-type p53 (wtp53) plays a key role in maintaining genomic stability and preventing cancer development, mutant p53 (mtp53) is not only deprived of the tumor-inhibitory activity but also endowed with oncogenic functions, leading to tumor growth and metastasis. mtp53 exerts the 'dominant-negative' effect on the remaining wild-type allele of *TP53* in cancer cells by impeding the

tetramerization and thus the transcriptional activity of wtp53. Importantly, mtp53 also endorses survival, proliferation, metastasis, metabolic adaptation, and microenvironment of cancer cells through 'gain-of-function' (GOF) mechanisms (Freed-Pastor and Prives, 2012; Stein et al., 2019; Zhou et al., 2019). Distinct working models are proposed for the acquired GOFs by mtp53 (Freed-Pastor and Prives, 2012; Zhou et al., 2019). Although most of the mtp53 proteins are unable to bind to the canonical p53-responsive DNA elements, they can transcriptionally regulate gene expression by interacting with other transcription factors or co-factors. For instance, mtp53-R175H can form a ternary complex with the transcription factor NF-Y and its co-factor p300 to induce the transcription of NF-Y target genes important for DNA synthesis and cell cycle progression (Di Agostino et al., 2006). Also, CDK4/cyclin D was recently shown to phosphorylate a liver cancer-derived hotspot p53 mutant, R249S, at this mutated amino acid (Ser) site, which in turn bound to c-Myc in the nucleus and augmented c-Myc-dependent ribosome biogenesis and cell proliferation (Liao et al.,

2017). In some cases, p53 mutants, such as R273P, can regulate gene transcription by directly associating with DNA, particularly with the specifically structured DNA, such as matrix attachment regions (MARs) (Will et al., 1998). In other scenarios, several p53 mutants, such as R248W and R273H, can bind to proteins unrelated to transcription and modulate their cellular functions (Song et al., 2007). Thereby, mtp53 can promote tumorigenesis and progression through various mechanisms.

Remarkably, one of the types of human cancer that harbor high frequent p53 mutations is ovarian cancer, as TP53 is mutated in >96% of the high-grade serous ovarian cancer (Cancer Genome Atlas Research Network, 2011; Patch et al., 2015). Because of this, mtp53 was considered a potential biomarker for ovarian malignancy and metastasis (Ren et al., 2016; Zhang et al., 2016). Some compounds, such as APR-246 and AZD1775, have been proved to be effective in the treatment of advanced and drug-refractory ovarian cancer by targeting mtp53 pathways (Bykov et al., 2002; Leijen et al., 2016). Given the critical role of mtp53 in supporting ovarian carcinogenesis, we sought to elucidate the underlying mechanisms by screening mtp53-interacting proteins in ovarian cancer tissues. We have recently found that the E3-ubiquitin ligase TRIM71 restrains ovarian carcinogenesis by interacting with mtp53 proteins, such as R273H and S241F, and inducing their proteasomal degradation (Chen et al., 2019). This screening also revealed B-cell CLL/lymphoma 7 protein family member C (BCL7C) as another potential mtp53-binding protein in ovarian cancer as further described below. The human BCL7 family proteins, including BCL7A, BCL7B, and BCL7C, share partial sequence identity in the N-terminal 51-amino acid region (Jadayel et al., 1998). Loss of BCL7A expression was found in multiple human cancers, owing to genetic alterations or promoter hypermethylation (Zani et al., 1996; van Doorn et al., 2005; Sun et al., 2019). BCL7B was shown to enhance apoptosis by negatively regulating the Wnt pathway in gastric cancer (Uehara et al., 2015), but to promote pancreatic cancer progression as an unfavorable prognostic marker (Taniuchi et al., 2018). Also, the BCL7 family proteins have been described as part of the SWI/SNF chromatin remodeling complexes (Kadoch et al., 2013). However, the biological function and clinical significance of BCL7C in cancer remain completely unknown.

In our attempt to determine the role of BCL7C in regulation of mtp53 in ovarian cancer, we found out that BCL7C expression is diminished in ovarian cancer compared with non-cancerous ovarian tissues, and its downregulation is associated with unfavorable prognosis of ovarian cancer. Also, we found that ectopic expression of BCL7C hampers, while knockdown of BCL7C boosts, ovarian cancer cell proliferation, and invasion. Interestingly, BCL7C interacted with mtp53 and repressed the expression of mtp53 target genes. Thus, our study as detailed below provides the first line of evidence showing that BCL7C may play a tumor-suppressive role in ovarian cancer by inactivating mtp53.

Results

Low level of BCL7C is associated with unfavorable prognosis in ovarian cancer

To explore the clinical relevance of BCL7C to ovarian cancer, we examined its expression in 5 non-cancerous and 11 cancerous ovarian specimens and found that BCL7C is underexpressed in ovarian cancer compared with the non-cancerous ovaries (Figure 1A). Consistently, the expression of BCL7C was significantly downregulated in different types of ovarian cancer by mining the Oncomine database (www.oncomine.org)
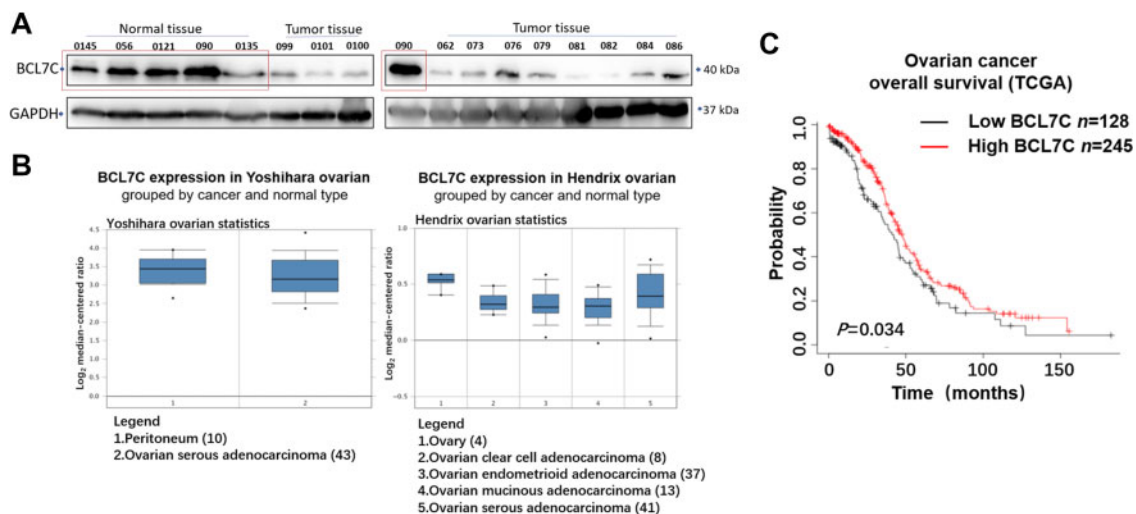
Figure 1 Underexpression of BCL7C in ovarian carcinoma is associated with unfavorable prognosis. (A) The expression of BCL7C is downregulated in ovarian cancer specimens vs. non-cancerous ovarian tissues. A total of 5 non-cancerous and 11 cancerous ovarian specimens were collected and subjected to IB analysis. (B) The expression of BCL7C is downregulated in ovarian cancer samples through bioinformatics analysis. The dots indicate the statistical outliers. (C) Lower expression level of BCL7C is associated with poor prognosis of ovarian cancer. All possible cutoff values between the lower and upper quartiles of BCL7C expression were computed, and the best performing threshold was used as a cutoff.

(Figure 1B). In addition, the Kaplan–Meier survival analysis (kmplot.com/analysis/) revealed that the higher level of BCL7C is associated with better prognosis of ovarian cancer (Figure 1C) as well as diverse human cancers, including cervical cancer, breast cancer, lung cancer, pheochromocytoma and paraganglioma, and thyroid cancer (Supplementary Figure S1). Taken together, these results suggest that BCL7C may play a tumor-suppressive role in ovarian cancer.

BCL7C impairs survival and proliferation of ovarian cancer cells harboring mtp53

Since the high level of BCL7C is associated with favorable prognosis (Figure 1C), we tested whether BCL7C is able to suppress ovarian cancer cell proliferation by performing a set of CCK-8 cell viability assays. To this end, two ovarian cancer cell lines, TOV112D and ES-2, were employed. TOV112D cells

sustain a hotspot mtp53-R175H, while ES-2 cells harbor a rarely studied mtp53-S241F that was recently shown to promote ovarian cancer cell growth and metastasis via its GOF activity (Chen et al., 2019). We introduced ectopic BCL7C or its specific siRNAs into the cells. As a result, ectopic BCL7C markedly inhibited proliferation of ES-2 cells (Figure 2A), while BCL7C ablation by two independent siRNAs drastically increased proliferation of ES-2 cells (Figure 2B). Also, knockdown of BCL7C in TOV112D cells boosted cell proliferation (Figure 2C). Furthermore, we determined whether BCL7C is required for apoptosis of the ovarian cancer cell line SKOV3 stably expressing a hotspot mtp53-R273H (Supplementary Figure S2K) by the flow cytometry analysis. Treatment of the cells with Cisplatin for 16 h dramatically increased apoptosis, whereas depletion of BCL7C by two independent siRNAs markedly attenuated Cisplatin-induced ovarian cancer cell apoptosis (Figure 2D). These effects were specific to dysregulation of BCL7C, as efficiency of BCL7C
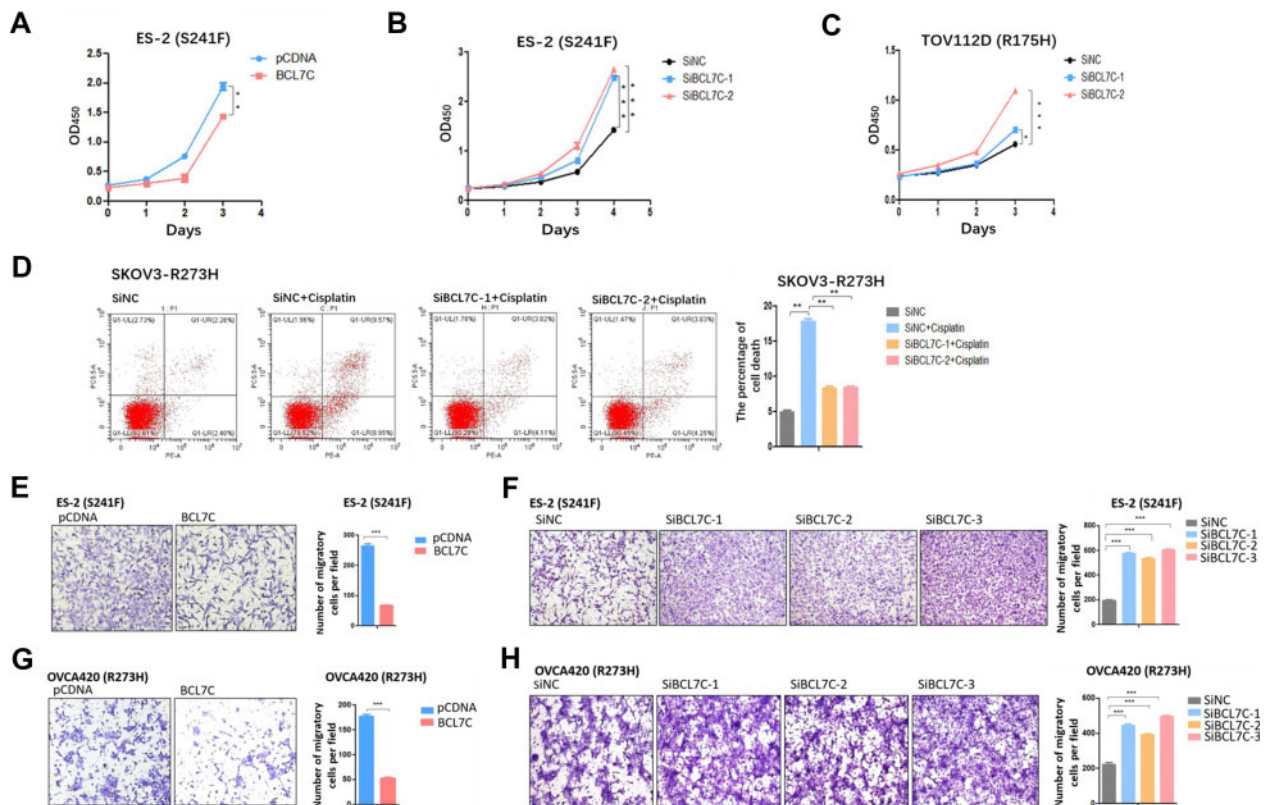
Figure 2 BCL7C inhibits ovarian cancer cell proliferation, survival, and invasion. (**A**) Ectopic BCL7C suppresses ovarian cancer cell proliferation. ES-2 cells were transfected with control or the BCL7C-encoding plasmid and subjected to the CCK-8 cell viability assay. (**B** and **C**) Knockdown of BCL7C accelerates ovarian cancer cell proliferation. ES-2 and TOV112D cells were transfected with control or BCL7C siRNA and subjected to the CCK-8 cell viability assay. (**D**) Knockdown of BCL7C inhibits Cisplatin-induced ovarian cancer cell apoptosis. mtp53-R273H-expressing SKOV3 cells were transfected with control or BCL7C siRNA for 48 h and subjected to the apoptotic Annexin V-FITC staining and flow cytometry analysis. Cisplatin was added into medium for 16 h before cells were harvested for apoptosis analysis. (**E**) Ectopic BCL7C constrains ovarian cancer cell invasion. ES-2 cells were transfected with control or the BCL7C-encoding plasmid for 24 h followed by the transwell cell invasion assay. (**F**) Knockdown of BCL7C induces ovarian cancer cell invasion. ES-2 cells were transfected with control or BCL7C siRNA for 24 h followed by the transwell cell invasion assay. (**G**) Ectopic BCL7C constrains invasion of the ovarian cancer cell line OVCA420. The same experiments as in **E** were performed except for using OVCA420 cells. (**H**) Knockdown of BCL7C induces invasion of the ovarian cancer cell line OVCA420. The same experiments as in **F** were performed except for using OVCA420 cells.

overexpression or depletion was validated in each cell line (Supplementary Figure S2). Therefore, these results demonstrate that BCL7C inhibits proliferation and induces apoptosis of ovarian cancer cells expressing mtp53.

BCL7C prohibits invasion of mtp53-containing ovarian cancer cells

Next, we determined whether BCL7C also affects ovarian cancer cell invasion. The transwell cell invasion assay was performed after introduction of ectopic BCL7C into ES-2 cells. As shown in Figure 2E, BCL7C overexpression constrained invasion of this cell line. Conversely, ablation of BCL7C by three independent siRNAs drastically bolstered invasion of ES-2 cells (Figure 2F). In agreement with the results, ectopic BCL7C profoundly inhibited invasion of ovarian cancer OVCA420 cells that harbor mtp53-R273H (Figure 2G), whereas knockdown of BCL7C enhanced invasion of the cells (Figure 2H). Altogether, the above results demonstrate that BCL7C can hamper proliferation and invasive of malignant ovarian cancer cells that harbor mtp53, suggesting a possible regulation of mtp53 as detailed below.

BCL7C interacts with various mtp53 proteins

In order to understand how BCL7C suppresses proliferation, survival, and invasion of ovarian cancer cells that harbor

mtp53 as shown above (Figure 2), we first determined whether BCL7C interacts with mtp53. This idea was in part supported by our recent screening for mtp53-binding proteins in primary ovarian cancer tissues (Chen et al., 2019), as that screening also revealed BCL7C as another possible mtp53-binding protein. To validate this result, we conducted a set of co-immunoprecipitation (co-IP)−immunoblotting (IB) analyses. As shown in Figure 3A, Myc-tagged BCL7C was co-immunoprecipitated with a variety of mtp53 proteins, including mtp53-R175H, mtp53-Y220C, mtp53-R248W, mtp53-R249S, and mtp53-R273H, by the anti-p53 antibody. This result was also verified by another set of reverse co-IP analyses with the anti-Myc antibody followed by IB assays (Figure 3B−F), indicating that ectopic BCL7C can bind to various exogenous mtp53s. This result was also confirmed for endogenous proteins, as endogenous BCL7C was co-immunoprecipitated with endogenous mtp53-R175H (Figure 3G), mtp53-S241F (Figure 3H), and mtp53-R273H (Figure 3I) in three ovarian cancer cell lines TOV112D, ES-2, and OVCA420, respectively. However, surprisingly, these interactions did not appear to affect the level (Supplementary Figure S3A) and cellular localization of these mtp53s (Supplementary Figure S3B−D). It was noted that BCL7C does not bind to wtp53 (Figure 3A), even when the level of endogenous wtp53 was induced by Cisplatin treatment for 24 h in ovarian cancer HEY cells (Figure 3J). Together, these
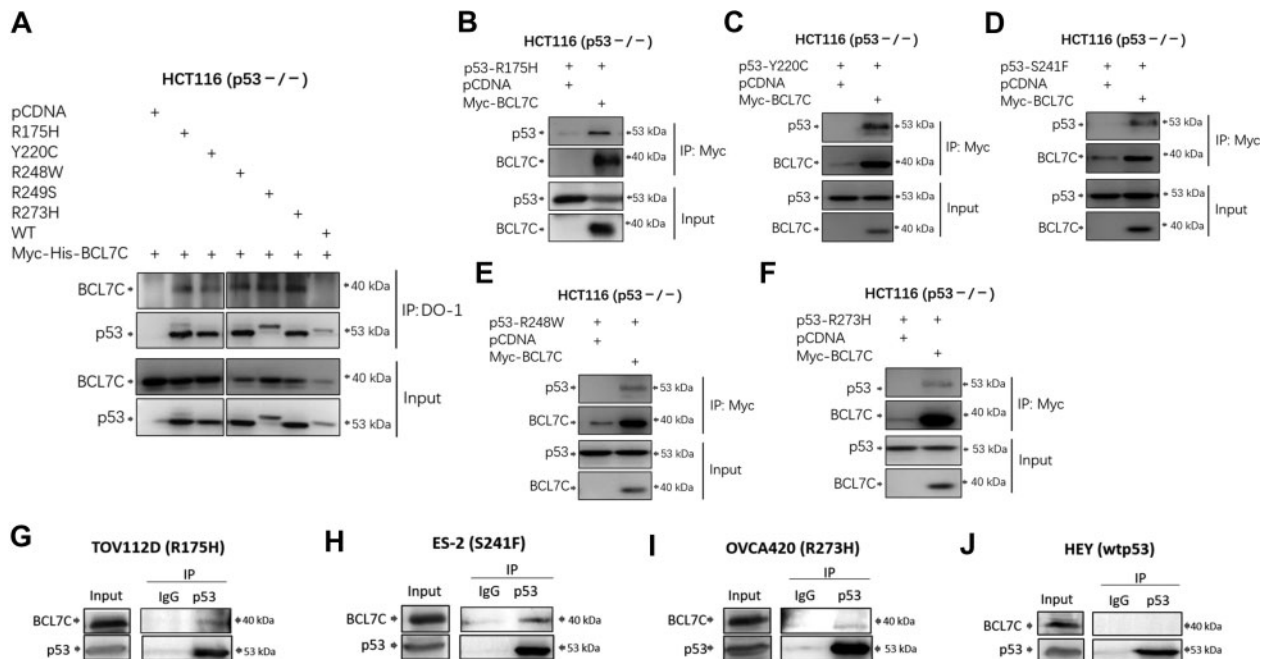
Figure 3 BCL7C interacts with mutant p53. (**A**) Myc-tagged BCL7C interacts with exogenous p53 mutants. HCT116$^{p53−/−}$ cells were transfected with the BCL7C-encoding plasmid along with control or different mtp53-encoding plasmids followed by co-IP−IB analyses using antibodies as indicated. (**B**−**F**) Exogenous interactions of BCL7C and p53 mutants are confirmed by reciprocal co-IP−IB analyses. HCT116$^{p53−/−}$ cells were transfected with combinations of plasmids encoding BCL7C and different p53 mutants followed by co-IP−IB analyses using antibodies as indicated. (**G**−**I**) Endogenous BCL7C binds to various endogenous p53 mutants in ovarian cancer cells. The ovarian cancer cell lines TOV112D, ES-2, and OVCA420, harboring mtp53-R175H, mtp53-S241F, and mtp53-R273H, respectively, were harvested for co-IP analysis using antibodies as indicated. (**J**) Endogenous BCL7C does not bind to endogenous wtp53. Ovarian cancer HEY cells harboring wtp53 were treated with Cisplatin for 24 h and harvested for co-IP analysis using antibodies as indicated.

results demonstrate that BCL7C can bind to all of the mtp53s tested in ovarian cancer cells, though it remains to find out what are the functional outcomes of these interactions.

BCL7C represses the expression of mtp53 target genes

Since ectopic BCL7C did not affect the level or cellular localization of mtp53 (Supplementary Figure S3), we wondered whether BCL7C influences mtp53 activity. Although point mutations occurring in the p53 DBD usually abrogate their DNA-binding ability, mtp53 proteins were found to indirectly bind to the transcription-associated DNA elements through interactions with different transcription factors or co-factors (Freed-Pastor and Prives, 2012; Zhou et al., 2019). Several of mtp53-responsive genes have been identified through these associations (Di Agostino et al., 2006; Bossi et al., 2008; Yan and Chen, 2009; Freed-Pastor et al., 2012). Thus, we tested whether BCL7C affects the expression of these direct or indirect target genes of mtp53 by performing quantitative reverse transcription–polymerase chain reaction (RT–qPCR) analysis following introduction of BCL7C into ES-2 and TOV112D cells. As shown in Figure 4A and B, ectopic BCL7C dramatically inhibited the expression of several mtp53 target genes, such as BUB1, CXCL1, c-MYC, MAP2K3, and NFKB2 required for cell survival and proliferation, as well as PXN, ITGA6, and MMP13 for EMT and metastasis (Freed-Pastor and Prives, 2012). By contrast, knocking down BCL7C by two independent siRNAs in ES-2 and TOV112D cells led to significant upregulation of multiple mtp53 target

genes, many of which are involved in cancer cell growth and metastasis (Figure 4C and D). In addition, we evaluated the correlation of BCL7C and mtp53 target genes in 11 ovarian cancer tissues described in Figure 1A. Based on the expression of BCL7C determined by RT–qPCR, the samples were stratified into two groups—three tumors with higher BCL7C expression and eight with lower BCL7C expression. Inversely proportional to the level of BCL7C, the expression of mtp53 target genes increased drastically in the ovarian cancer tissues sustaining minimal expression of BCL7C (Figure 4E), suggesting that loss of BCL7C is associated with enhanced mtp53 transcriptional activity leading to the development of ovarian carcinoma.

BCL7C suppresses ovarian cancer propagation dependent on mtp53

Next, we tested whether BCL7C represses mtp53 target gene expression by directly inactivating mtp53 or through other transcription factors. The expression of multiple mtp53 target genes was evaluated in two isogenic cell lines, SKOV3 and mtp53-R273H-expressing SKOV3. We showed that ablation of BCL7C does not modulate the expression of mtp53 target genes in SKOV3 cells (Figure 5A) whereas significantly induces their expression in mtp53-R273H-expressing SKOV3 cells (Figure 5B). To further determine whether the tumor-inhibitory effect of BCL7C is through regulation of mtp53, we employed the p53-negative cell lines, SKOV3 and HCT116$^{p53-/-}$, as well as the wtp53-expressing A2780 cell line. Knockdown of BCL7C
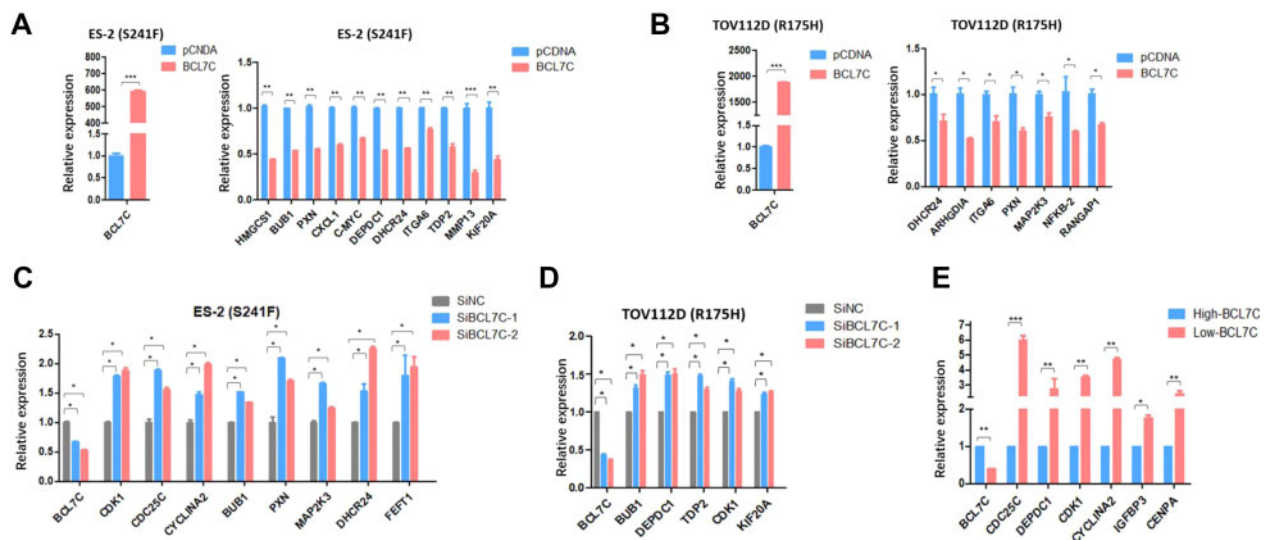
Figure 4 BCL7C represses ovarian carcinoma by inhibiting mtp53 target gene expression. (**A**) Ectopic BCL7C represses mtp53 target gene expression in ES-2 cells. Cells were transfected with control or the BCL7C-encoding plasmid for 48 h followed by RT–qPCR analysis. (**B**) Ectopic BCL7C represses mtp53 target gene expression in TOV112D cells. The same experiments as in **A** were performed except for using the TOV112D cell line. (**C**) Knockdown of BCL7C elevates mtp53 target gene expression in ES-2 cells. Cells were transfected with control or BCL7C siRNA for 48 h followed by RT–qPCR analysis. (**D**) Knockdown of BCL7C elevates mtp53 target gene expression in TOV112D cells. The same experiments as in **C** were performed except for using the TOV112D cell line. (**E**) BCL7C is negatively correlated with the expression of mtp53 target genes in ovarian cancer samples. A total of 11 cancerous ovarian specimens as described in Figure 1A were subjected to RT–qPCR analysis.
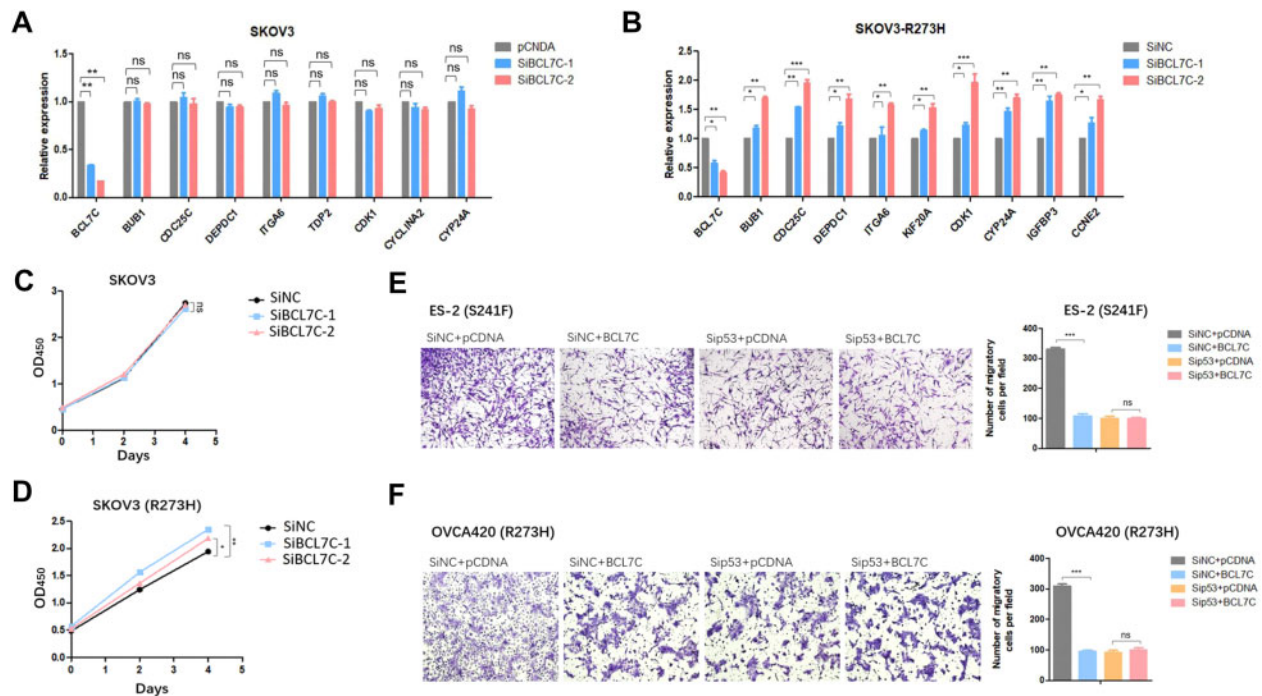
Figure 5 BCL7C suppresses ovarian cancer cell proliferation and invasion through inactivation of mtp53. (**A**) Knockdown of BCL7C does not affect mtp53 target gene expression in SKOV3 cells. Cells were transfected with control or BCL7C siRNA for 48 h followed by RT–qPCR analysis. (**B**) Knockdown of BCL7C significantly increases mtp53 target gene expression in mtp53-R273H-expressing SKOV3 cells. Cells were transfected with control or BCL7C siRNA for 48 h followed by RT–qPCR analysis. (**C**) Knockdown of BCL7C does not affect SKOV3 cell proliferation. Cells were transfected with control or BCL7C siRNA followed by CCK-8 cell viability analysis. (**D**) Knockdown of BCL7C significantly induces proliferation of mtp53-R273H-expressing SKOV3 cells. Cells were transfected with control or BCL7C siRNA followed by CCK-8 cell viability analysis. (**E** and **F**) BCL7C suppresses ovarian cancer cell invasion in a mtp53-dpendent manner. ES-2 (**E**) or OVCA420 (**F**) cells were transfected with combinations of the plasmids and siRNA as indicated for 24 h, followed by the transwell cell invasion assay.

in any of the three cell lines barely affected cell proliferation (Figure 5C; Supplementary Figure S4A and B). Interestingly, BCL7C gained the ability to effectively regulate proliferation of HCT116$^{p53-/-}$ and SKOV3 cells that were transiently or stably transfected with the plasmid encoding mtp53 (Figure 5D; Supplementary Figure S4C and D). Additionally, ectopic BCL7C markedly inhibited ES-2 cell invasion but had no influence on invasion of the cells with depleted mtp53 by siRNA (Figure 5E). Moreover, BCL7C was also shown to suppress invasion of OVCA420 cells in a mtp53-dependent fashion, as depletion of mtp53 completely abrogated the ability of BCL7C to suppress invasion (Figure 5F). These effects were specific to deregulation of the BCL7C–mtp53 axis, as efficiency of BCL7C overexpression and mtp53 depletion was validated (Supplementary Figure S2L and M). Collectively, our findings convincingly demonstrate that BCL7C plays a tumor-suppressive role in ovarian cancer cells by inhibiting mtp53 activity.

Discussion

TP53 mutation is the most frequent event of genomic alterations during the development of human ovarian carcinoma (Zhang et al., 2016). Thus, better understanding why and how this event highly occurs in ovarian carcinoma would provide

useful information for the improvement of therapies and prognosis for this type of cancer. Through our effort in doing so, we identified BCL7C as a new potential mtp53-binding protein. Indeed, our further studies as described here confirmed its interaction with various hotspot p53 mutants (Figure 3A–I). Also, our biochemical experiments demonstrated that ectopically expressed BCL7C can inhibit the transcriptional activity of these mtp53s (Figure 4A and B), while knockdown of this protein leads to the higher expression of a number of mtp53 target genes as tested here (Figures 4C, D and 5B). Consistent with these results, ectopic BCL7C can suppress mtp53-dependent survival, proliferation, and invasion of ovarian cancer cells (Figures 2 and 5; Supplementary Figure S4). These results suggest that BCL7C might act as a tumor suppressor in ovarian cancer.

BCL7C, along with BCL7A and BCL7B, belongs to the B-cell CLL/lymphoma 7 protein family. These members of the family appear to play different roles in oncogenesis. BCL7A was suggested as a tumor suppressor, as it was frequently mutated, deleted, or downregulated in human cancers (Zani et al., 1996; van Doorn et al., 2005; Sun et al., 2019), while the function of BCL7B in cancer remains debated. On the one hand, BCL7B was found to reside in the region of 7q11.23, which is

commonly deleted in the Williams syndrome-associated lymphoma (Amenta et al., 2004; Zhukova and Naqvi, 2013). Consistently, BCL7B was able to maintain the nuclear structure and to prevent tumorigenesis by inducing apoptosis (Uehara et al., 2015). On the other hand, BCL7B was reported to play an oncogenic part in pancreatic cancer (Taniuchi et al., 2018, 2019). Genetically, the single and double knockout mouse models for murine Bcl7a and Bcl7b revealed that the two genes do not have redundant or overlapping roles during embryonic development (Wischhof et al., 2017). Structurally, they show minimum homology except for their N-terminal conserved 51-amino acid sequence (Jadayel et al., 1998). However, little is known about biochemical and physiological functions of BCL7C. Therefore, our study as presented here reveals for the first time the anti-cancer function of BCL7C by suppressing mtp53 activity.

The anti-cancer role of BCL7C is also supported by the following findings. First, comparison of expression patterns of BCL7C between non-cancerous and cancerous ovarian tissues revealed that BCL7C protein level dramatically declines in ovarian cancer (Figure 1A). This was further verified at the mRNA level by RT–qPCR analysis of the ovarian specimens and by mining the information from the Oncomine database (Figure 1B). Because BCL7C is located at chromosome 16p11.2 that is not related to any cancer-associated deletion or rearrangements (Jadayel et al., 1998), and no mutation has been found in this gene from the TCGA database, the expression of BCL7C in ovarian cancer must be repressed through transcriptional control or epigenetic modifications. Consistent with the clinical dataset, BCL7C can inhibit ovarian cancer cell growth and invasion (Figure 2) but has minimum effect on cancer cells without mtp53 (Figure 5; Supplementary Figure S4), suggesting that the anti-cancer activity of BCL7C is through repression of mtp53 in ovarian cancer. mtp53 is associated with resistance of cancer cells to chemotherapeutic drugs by upregulating the expression of survival genes, such as c-MYC, NFKB2, and TDP2 (Freed-Pastor and Prives, 2012; Zhou et al., 2019). Our results showed that depletion of BCL7C dramatically impairs ovarian cancer cell apoptosis induced by Cisplatin, implying that BCL7C may also play a role in suppressing mtp53-mediated chemoresistance. Another interesting finding is that BCL7C is positively associated with prognosis of numerous human cancers (Figure 1C; Supplementary Figure S1). Among these cancers, cervix and thyroid carcinomas usually sustain much fewer TP53 mutations (Leroy et al., 2014). Thus, these findings not only support the anti-cancer role of BCL7C in mtp53-dependent oncogenesis in certain types of cancers, such as ovarian cancer, but also suggest the mtp53-independent anti-cancer activity of this protein in other types of cancers.

Through our initial co-IP–mass spectrometry analysis, we identified BCL7C as one of the potential interacting proteins of p53-S241F, which is present at a relatively high frequency in ovarian cancer (Chen et al., 2019). However, surprisingly, our further studies showed that BCL7C could actually bind to all of the mtp53 proteins as examined here, including mtp53-R175H,

mtp53-Y220C, mtp53-S241F, mtp53-R248W, mtp53-R249S, and mtp53-R273H (Figure 3), though it remains to investigate how BCL7C prefers to binding to these mtp53s over their wild-type counterpart. Also, ectopic BCL7C suppressed the expression of a broad spectrum of mtp53 target genes (Figures 4A–D and 5B). Although most of the target genes are responsible for cancer cell growth and metastasis, some are involved in metabolism. For instance, HMGCS1 and DHCR24 are involved in cholesterol biogenesis (Freed-Pastor et al., 2012), and DEPDC1 is involved in the regulation of GTPase activity (Girardini et al., 2011). This result is in line with the concept that perturbation of cancer cell metabolism by confining expression of these genes leads to the restriction of tumor growth and propagation (Girardini et al., 2011; Freed-Pastor et al., 2012). These results were confirmed by the inverse correlation of the expression of BCL7C and mtp53 target genes in ovarian carcinomas (Figure 4E). Hence, once again, our study further verifies the anti-cancer role of BCL7C by inhibiting various mtp53 functions in ovarian cancer.

In our attempt to elucidate other possible molecular mechanisms underlying the regulation of mtp53 by BCL7C, we learned that BCL7C has no impact on the protein expression or cellular localization of mtp53s (Supplementary Figure S3). Thus, downregulation of mtp53 target genes by BCL7C (Figures 4A–D and 5B) suggests that inhibition of mtp53 transcriptional activity via direct interaction appears to be the main mechanism for the inactivation of the mtp53 oncogenic functions by this tumor suppressor. This conjecture is in accordance with studies by others. A plethora of mechanisms underlying the GOFs of different p53 mutants have been reported (Freed-Pastor and Prives, 2012; Muller and Vousden, 2014; Zhou et al., 2019). For example, both mtp53-R175H and mtp53-R273H can interact with NF-Y to boost cancer cell proliferation (Di Agostino et al., 2006). mtp53-R175H was found to empower TGF-β-mediated cancer cell metastasis by connecting the TGF-β:Smad cascade with TAp63 (Adorno et al., 2009), while mtp53-R273H preferentially associates with SREBP-2 to promote tumor survival and metastasis via the mevalonate pathway (Freed-Pastor et al., 2012). Thus, it still remains to further interrogate whether BCL7C interferes with the binding of mtp53 to those oncogenic transcriptional factors or co-factors, consequently leading to the inhibition of mtp53 activity, which will be an enticing topic for our future study.

In conclusion, our results as described above demonstrate that the under-studied BCL7 family member, BCL7C, can function as a tumor suppressor in ovarian cancer by targeting mtp53s. This statement is supported by the following lines of evidence: (i) the level of BCL7C is markedly reduced in ovarian carcinoma specimens compared with non-cancerous ovarian tissues; (ii) the higher level of BCL7C is well correlated with better prognosis of ovarian cancer; (iii) BCL7C suppresses ovarian cancer cell growth and invasion, while its knockdown reverses these cellular events; (iv) BCL7C can interact with various p53 mutants and suppresses their oncogenic GOFs by downregulating mtp53 target gene expression in ovarian cancer cells. Therefore, our study

identifies BCL7C as a new negative regulator of hotspot mtp53s. Further dissecting its detailed mechanisms of action on mtp53s and investigating its biological role in ovarian cancer development are the topics for our future studies.

Materials and methods

Cell culture and transient transfection

Human ovarian cancer cell lines, ES-2, OVCA420, TOV112D, HEY, A2780, and SKOV3, and the colon cancer cell line HCT116$^{p53-/-}$ were cultured in Dulbecco's modified Eagle's medium supplemented with 10% fetal bovine serum, 100 U/ml penicillin, and 100 μg/ml streptomycin. All cells were cultured at 37°C in an incubator containing 5% carbon dioxide. Cells were seeded in Petri dishes at appropriate density 1 day before transfection according to the manufacturer's protocol of the Hieff Trans liposomal transfection reagent (Yeasen). Cells were then collected or split for future experiments 24–48 h post-transfection. The proteasome inhibitor MG132 (Sigma-Aldrich) was added 4–6 h before cells were harvested for IP.

Plasmids and antibodies

The Flag-tagged BCL7C-expressing plasmid was purchased from Vigene Biosciences, Inc. The Myc-tagged BCL7C plasmid was generated by inserting the full-length cDNA amplified by PCR into the pcDNA3.1/Myc-His vector between the *Xho*I and *Nhe*I sites, using the primers 5′-CTAGCTAGCATGGCCGG CCGGACTGTA-3′ and 5′-CCCTCGAG TGGGGTCAGGGGCATT TGGGCAGAT-3′. The plasmids encoding non-tagged mtp53s (R175H, Y220C, S241F, R248W, R249S, and R273H) were generated as previously described (Chen et al., 2019). The anti-Myc (Catalog No. 60003-1, Proteintech), anti-p53 (DO-1, Catalog No. sc-126, Santa Cruz Biotechnology), anti-BCL7C (Catalog No. 126944, Abcam), anti-α-Tubulin (Catalog No. 66031-1, Proteintech), anti-Histone-H3 (Catalog No. 17168-1, Proteintech), anti-GAPDH (Catalog No. 60004-1, Proteintech), the secondary antibodies for rabbit (Catalog No. ARG65351, Arigo) and mouse (Catalog No. ARG65350, Arigo), and the light chain-specific secondary mouse antibody (Catalog No. 115-035-174, Jackson) were commercially purchased.

Reverse transcription and RT–qPCR analyses

Total RNA from cells or human tissues were prepared by using RNAiso Plus (TaKaRa) according to the manufacturer's protocol. cDNA was prepared by using the PrimeScript RT reagent Kit with gDNA Eraser (TaKaRa). RT–qPCR was conducted using TB Green Premix following the manufacturer's protocol (TaKaRa). The primers for BCL7C, p53, mtp53 targeting genes including HMGCS1, BUB1, CXCL1, c-MYC, DEPDC1, ITGA6, TDP2, MMP13, KIF20A, NFKB2, RANGAP1, ARHGDIA, MAP2K3, CDK1, CDC25C, CYCLINA2, FDFT1, CCNE2, and CENPA, and GAPDH are as follows:

BCL7C, 5′-CGGCTGGGCCAAGAGAG-3′ and 5′-AGCAGTTCTGG AACAGGCTC-3′; p53, 5′-CCCAAGCAATGGATGATTTGA-3′ and 5′-GGCATTCTGGGAGCTTCATCT-3′; HMGSCS1, 5′-GGGCAGGGCATTAT TAGGCTAT-3′ and 5′-TTAGGTTGTCAGCCTCTATGTTGAA-3′; BUB1, 5′-ATTCAAGCCACAGAGTGGAGCAG-3′ and 5′-AGAACTTGTGTT GGCAACCTTATGTG-3′; PXN, 5′-GGCTCTCCGTGCTCCCGAGTG-3′ and 5′-GCAGCAGGCGGTCGAGTT-3′; CXCL1, 5′-CTGAACAGTG ACAAATCCAAC-3′ and 5′-CCTAAGCGATGCTCAAACAC-3′; c-MYC, 5′-GGAGATCCGGAGCGAATAG-3′ and 5′-CCTTGCTCGGGTGTTGTA AGT-3′; DEPDC1, 5′-TGGGTATTATCTGCCATGAAGTGCCT-3′ and 5′-AGGTTGCAGCAAGCCCAAAATGT-3′; DHCR24, 5′-CAAGTACGGCCT GTTCCAACA-3′ and 5′-CGCACAAAGCTGCCATCA-3′; ITGA6, 5′-GCACGCGGATCGAGTT-3′ and 5′-CTCGGGATTCCTGCTTCGTAT-3′; TDP2, 5′-ATGCTGCGGAACGAATGAAT-3′ and 5′-CCACCACATCTG GTAACCTCTC-3′; MMP13, 5′-GAATTAAGGAGCATGGCGACT-3′ and 5′-CTAAGGAGTGGCCGAACT-3′; KIF20A, 5′-TCCTCAAGGAGTCACT GACAAG-3′ and 5′-GATGGGCCACTGACTGTTGT-3′; NFKB2, 5′-GGGGCATCAAACCTGAAGATTTCT-3′ and 5′-TCCGGAACACAATG GCATACTGT-3′; RANGAP1, 5′-GCTCCAAGGGTGCAGTTG-3′ and 5′-GCAGCATCCCTCTTGATTTC-3′; ARHGDIA, 5′-AGCCTGCGAAAGTA CAAGGA-3′ and 5′-GGTCAGGCCAGTCACCAC-3′; MAP2K3, 5′-CTGCGGTTCCCTTACGAGT-3′ and 5′-GCAATGTCCGTCTTCTTGGT-3′; CDK1, 5′-CCTTGCCAGAGCTTTTGGAATACC-3′ and 5′-GACATGGGAT GCTAGGCTTCCTGG-3′; CDC25C, 5′-GTATCTGGGAGGACACATCCA GGG-3′ and 5′-CAAGTTGGTAGCCTGTTGGTTTG-3′; CYCLINA2, 5′AGCAGCCTGCAAACTGCAAAGTTG-3′ and 5′TGGTGGGTTGAGGA GAGAAACAC-3′; FDFT1, 5′-TCAGACCAGTCGCAGTTTCG-3′ and 5′-CTGCGTTGCGCATTTCC-3′; CCNE2, 5′-TGAGCCGAGCGGTAGCTGGT-3′ and 5′-GGGCTGGGGCTGCTGCTTAG-3′; CENPA, 5′-CTTCCT CCCATCAACACAGTCG-3′ and 5′-TGCTTCTGCTGCCTCTTGTAGG-3′; GAPDH, 5′-GGAGCGAGATCCCTCCAAAAT-3′ and 5′-GGCTGTTGTC ATACTTCTCATGG-3′.

Generating stable cell lines

The pLenti-EF1a-EGFP-F2A-Puro-CMV lentiviral plasmids encoding mtp53-R273H or the empty vector were packaged and purified as described (OBio Technology). SKOV3 cells were infected with appropriate amount of virus for overnight and then the medium was changed. The stable cells were selected with 1 μg/ml puromycin.

IB

Cells were harvested, lysed using lysis buffer (50 mM Tris/HCl (pH 7.5), 0.5% Nonidet P-40 (NP-40), 1 mM ethylenediaminetetraacetic acid, 150 mM NaCl, 1 mM dithiothreitol, 0.2 mM phenylmethylsulfonyl fluoride, 10 mM pepstatin A, and 1 mM leupeptin), and incubated on ice for 45–60 min. Equal amounts of clear cell lysate were used for IB analysis.

Co-IP

Clear cell lysates were aliquoted for input samples before being used for the co-IP assay. A total of 800–1000 μg proteins were incubated with the indicated antibodies at 4°C for 4 h or overnight. Protein G beads (Santa Cruz Biotechnology) were then added to the mixture and incubate at 4°C for additional

1–2 h. Beads were washed with cold lysis buffer at least three times. Bound proteins and input samples were analyzed by IB.

Immunofluorescence staining and confocal microscopy

The immunofluorescence staining assay was performed as previously described (Hao et al., 2020). Briefly, cells were fixed with methanol at $-20°C$ for overnight, and then washed by phosphate-buffered saline (PBS) and blocked with 8% bovine serum albumin (BSA) in PBS for 1 h followed by incubation with primary antibodies (anti-Myc, 1:300 dilution; anti-p53, 1:300 dilution) in 2% BSA in $4°C$ for overnight. The cells were then washed and incubated with the corresponding secondary antibodies and DAPI. Images were acquired with a confocal microscope (Leica SP5).

RNA interference

The siRNAs were synthesized and purified by GenePharma. The siRNA sequences against human BCL7C are 5′-GATCT TAATGATGAGAACA-3′ (si-BCL7C-1), 5′-AAGCTTACCCTGTCTTTGA-3′ (si-BCL7C-2), and 5′-CCAGAGTTTCCATTCGGAA-3′ (si-BCL7C-3). The siRNA sequence against human p53 is 5′-GUAAUCUACUG GGACGGAAtt-3′ (si-p53) as previously described (Zhou et al., 2016). siRNAs of 50–100 nM were transfected into cells using the Hieff Trans liposomal transfection reagent according to the manufacturer's protocol (Yeasen). Cells were harvested at 48–72 h after transfection for future experiments.

Cell viability assay

Long-term cell survival was assessed using the Cell Counting Kit-8 (CCK-8) (Dojindo) according to the manufacturer's instructions. Cells were seeded into 96-well plates with 1500 cells in 100 µl DMEM per well at 24 h after transfection. Then, 10 µl of WST-8 was added into each well for 2 h and cell viability was determined every 24 h using a Microplate Reader at the absorbance of 450 nm.

Flow cytometry analysis

The FITC Annexin V Apoptosis Detection Kit I (BD Biosciences) was used for apoptosis analysis according to the manufacturer's instruction. Briefly, cells were washed twice with cold PBS, resuspended in binding buffer, and stained with FITC Annexin V and PI for 15 min at room temperature. The cells were then analyzed by a FC500 MPL flow cytometer (Beckham Coulter).

Cell invasion assay

The invasion assay was performed as previously described (Chen et al., 2019). In brief, 5×10^4 cells suspended in 100 µl of serum-free medium were added to the upper chamber. The lower chambers were filled with the normal culture medium. After culture for 24 h at $37°C$, the cells on the upper surface were scraped and washed away, and the cells on the lower surface were fixed with methanol and stained with 0.1% crystal violet. The number of invaded cells was counted in at least three randomly selected fields under an optical microscope by image J software.

Fractionation of cell components

Cells were gently resuspended in 400 µl cell lysis buffer A (10 mM HEPES, 10 mM NaCl, 0.1 mM EDTA, 0.1 mM EGTA, 1 mM DTT, 1 mM PMSF, and the protease inhibitor cocktail) by pipetting up and down several times and incubated on ice for 10 min, followed by addition of 12.5 µl detergent (10% NP-40) and vortexing for 10 sec at the highest setting. The homogenate was centrifuged at $4°C$ and the supernatant that contains the cytoplasmic fraction was collected. The pellet was resuspended in 40 µl lysis buffer B (20 mM HEPES, 400 mM NaCl, 1 mM EDTA, 1 mM EGTA, 1 mM DTT, 1 mM PMSF, and the protease inhibitor cocktail) and incubated on ice for 30 min with vortexing at every 5 min. The homogenate was centrifuged at $4°C$ and the supernatant that contains the nuclear fraction was collected. The cytoplasmic and nuclear fractions were then analyzed by IB.

Human ovarian specimens

Tissue samples were obtained from patients undergoing gynecological and obstetric surgery at Xiangya Hospital of Central South University. They were classified as patients with advanced ovarian cancer stages III and IV according to Figo guidelines and the pathological type was high-grade serous ovarian cancer. Non-cancerous ovarian tissues were derived from non-ovarian cancer patients, or one side normal ovarian tissues of the patients with early-stage ovarian cancer. Fresh tissue samples were collected from ovarian cancer surgery. After surgically removed, the samples were immediately aliquoted, placed into liquid nitrogen, and then transferred to $-80°C$ refrigerator for long-term storage. Informed consent was obtained from all patients, and the study was approved by the Ethics Committee of Xiangya Hospital of Central South University.

Database of cancer patients

The expression of BCL7C in cancerous vs. normal ovarian tissues was analyzed through the Oncomine database (www.onco mine.org). Cancer patient survival was analyzed by the Kaplan–Meier method using the KM plotter database (kmplot.com/analysis/) (Nagy et al., 2018).

Statistics

The Student's *t*-test or one-way analysis of variance was performed to evaluate the differences between two groups or more than two groups. The Kaplan–Meier statistics were used to analyze the significant difference of patient survival. $P < 0.05$ was considered statistically significant, and asterisks represent significance in the following way: $*P < 0.05$, $**P < 0.02$, and $***P < 0.01$. Quantitative data are presented as mean $\pm$ SD.

Supplementary material

Acknowledgements

Funding

Conflict of interest: none declared.

Author contributions: C.H. and Q.H. conducted the studies and analyzed the data; Q.H. designed part of the studies. G.S. provided part of critical experimental materials; X.Z. and Y.Z. designed the studies, analyzed the data, and composed the manuscript.

References

Adorno, M., Cordenonsi, M., Montagner, M., et al. (2009). A mutant-p53/Smad complex opposes p63 to empower TGFβ-induced metastasis. Cell *137*, 87–98.

Amenta, S., Moschovi, M., Sofocleous, C., et al. (2004). Non-Hodgkin lymphoma in a child with Williams syndrome. Cancer Genet. Cytogenet. *154*, 86–88.

Bossi, G., Marampon, F., Maor-Aloni, R., et al. (2008). Conditional RNA interference in vivo to study mutant p53 oncogenic gain of function on tumor malignancy. Cell Cycle *7*, 1870–1879.

Bykov, V.J., Issaeva, N., Shilov, A., et al. (2002). Restoration of the tumor suppressor function to mutant p53 by a low-molecular-weight compound. Nat. Med. *8*, 282–288.

Cancer Genome Atlas Research Network. (2011). Integrated genomic analyses of ovarian carcinoma. Nature *474*, 609–615.

Chen, Y., Hao, Q., Wang, J., et al. (2019). Ubiquitin ligase TRIM71 suppresses ovarian tumorigenesis by degrading mutant p53. Cell Death Dis. *10*, 737.

Di Agostino, S., Strano, S., Emiliozzi, V., et al. (2006). Gain of function of mutant p53: the mutant p53/NF-Y protein complex reveals an aberrant transcriptional mechanism of cell cycle regulation. Cancer Cell *10*, 191–202.

Freed-Pastor, W.A., and Prives, C. (2012). Mutant p53: one name, many proteins. Genes Dev. *26*, 1268–1286.

Freed-Pastor, W.A., Mizuno, H., Zhao, X., et al. (2012). Mutant p53 disrupts mammary tissue architecture via the mevalonate pathway. Cell *148*, 244–258.

Girardini, J.E., Napoli, M., Piazza, S., et al. (2011). A Pin1/mutant p53 axis promotes aggressiveness in breast cancer. Cancer Cell *20*, 79–91.

Hao, Q., Wang, J., Chen, Y., et al. (2020). Dual regulation of p53 by the ribosome maturation factor SBDS. Cell Death Dis. *11*, 197.

Jadayel, D.M., Osborne, L.R., Coignet, L.J., et al. (1998). The BCL7 gene family: deletion of BCL7B in Williams syndrome. Gene *224*, 35–44.

Kadoch, C., Hargreaves, D.C., Hodges, C., et al. (2013). Proteomic and bioinformatic analysis of mammalian SWI/SNF complexes identifies extensive roles in human malignancy. Nat. Genet. *45*, 592–601.

Leijen, S., van Geel, R.M., Sonke, G.S., et al. (2016). Phase II study of WEE1 inhibitor AZD1775 plus carboplatin in patients with TP53-mutated ovarian cancer refractory or resistant to first-line therapy within 3 months. J. Clin. Oncol. *34*, 4354–4361.

Leroy, B., Anderson, M., and Soussi, T. (2014). TP53 mutations in human cancer: database reassessment and prospects for the next decade. Hum. Mutat. *35*, 672–688.

Liao, P., Zeng, S.X., Zhou, X., et al. (2017). Mutant p53 gains its function via c-Myc activation upon CDK4 phosphorylation at serine 249 and consequent PIN1 binding. Mol. Cell *68*, 1134–1146.e6.

Muller, P.A., and Vousden, K.H. (2014). Mutant p53 in cancer: new functions and therapeutic opportunities. Cancer Cell *25*, 304–317.

Nagy, A., Lanczky, A., Menyhart, O., et al. (2018). Validation of miRNA prognostic power in hepatocellular carcinoma using expression data of independent datasets. Sci. Rep. *8*, 9227.

Patch, A.M., Christie, E.L., Etemadmoghadam, D., et al. (2015). Whole-genome characterization of chemoresistant ovarian cancer. Nature *521*, 489–494.

Ren, Y.A., Mullany, L.K., Liu, Z., et al. (2016). Mutant p53 promotes epithelial ovarian cancer by regulating tumor differentiation, metastasis, and responsiveness to steroid hormones. Cancer Res. *76*, 2206–2218.

Song, H., Hollstein, M., and Xu, Y. (2007). p53 gain-of-function cancer mutants induce genetic instability by inactivating ATM. Nat. Cell Biol. *9*, 573–580.

Stein, Y., Aloni-Grinstein, R., and Rotter, V. (2019). Mutant p53—a potential player in shaping the tumor–stroma crosstalk. J. Mol. Cell Biol. *11*, 600–604.

Sun, Z., Sun, L., He, M., et al. (2019). Low BCL7A expression predicts poor prognosis in ovarian cancer. J. Ovarian Res. *12*, 41.

Taniuchi, K., Furihata, M., Naganuma, S., et al. (2018). BCL7B, a predictor of poor prognosis of pancreatic cancers, promotes cell motility and invasion by influencing CREB signaling. Am. J. Cancer Res. *8*, 387–404.

Taniuchi, K., Furihata, M., Naganuma, S., et al. (2019). Overexpression of PODXL/ITGB1 and BCL7B/ITGB1 accurately predicts unfavorable prognosis compared to the TNM staging system in postoperative pancreatic cancer patients. PLoS One *14*, e0217920.

Uehara, T., Kage-Nakadai, E., Yoshina, S., et al. (2015). The tumor suppressor BCL7B functions in the Wnt signaling pathway. PLoS Genet. *11*, e1004921.

van Doorn, R., Zoutman, W.H., Dijkman, R., et al. (2005). Epigenetic profiling of cutaneous T-cell lymphoma: promoter hypermethylation of multiple tumor suppressor genes including BCL7a, PTPRG, and p73. J. Clin. Oncol. *23*, 3886–3896.

Will, K., Warnecke, G., Wiesmuller, L., et al. (1998). Specific interaction of mutant p53 with regions of matrix attachment region DNA elements (MARs) with a high potential for base-unpairing. Proc. Natl Acad. Sci. USA *95*, 13681–13686.

Wischhof, L., Maida, S., Piazzesi, A., et al. (2017). The SWI/SNF subunit Bcl7a contributes to motor coordination and Purkinje cell function. Sci. Rep. *7*, 17055.

Yan, W., and Chen, X. (2009). Identification of GRO1 as a critical determinant for mutant p53 gain of function. J. Biol. Chem. *284*, 12178–12187.

Zani, V.J., Asou, N., Jadayel, D., et al. (1996). Molecular cloning of complex chromosomal translocation t(8; 14; 12)(q24.1; q32.3; q24.1) in a Burkitt lymphoma cell line defines a new gene (BCL7A) with homology to caldesmon. Blood *87*, 3124–3134.

Zhang, Y., Cao, L., Nguyen, D., et al. (2016). TP53 mutations in epithelial ovarian cancer. Transl. Cancer Res. *5*, 650–663.

Zhou, X., Hao, Q., Liao, P., et al. (2016). Nerve growth factor receptor negates the tumor suppressor p53 as a feedback regulator. eLife *5*, e15099.

Zhou, X., Hao, Q., and Lu, H. (2019). Mutant p53 in cancer therapy—the barrier or the path. J. Mol. Cell Biol. *11*, 293–305.

Zhukova, N., and Naqvi, A. (2013). Williams–Beuren syndrome and Burkitt leukemia. J. Pediatr. Hematol. Oncol. *35*, e30–e32.